Corrosion Behavior of Austenitic Stainless Steel Used in Nuclear Power Plant Cooling Water Component After Plasma Electrolytic Oxidation

Jun Heo[a], Seunguk Cheon[a], and Sung Oh Cho[a*]
Department of Nuclear and Quantum Engineering, Korea Advanced Institute of Science and Technology (KAIST), Daejeon 34141, Korea
[*]Corresponding author: socho@kaist.ac.kr

1. Introduction

Stainless steel (SS) is widely used in various industrial fields due to its excellent properties including corrosion resistance, good ductility, and being readily formable. Also, its remarkable mechanical strength, weldability, and high performance at all temperatures are additional advantages. The typical types of SS used in industries are 304(L) and 316(L) type SS. In nuclear power plants, various components adopt stainless steel as a structural material. Tube support plates in the secondary loop of the steam generator, turbine blade, moisture separator, and seawater lift pumps are the representative components using stainless steel.

All that noted, the secondary and tertiary loops of the nuclear power plant involve corrosive and abrasive particles. With secondary side cooling water, high temperature and pressure with dissolved oxygen and pH-controlling additives form the corrosive environments for structural materials. In the case of the tertiary loop which uses seawater as a coolant exhibits highly corrosive and abrasive environments as well due to the high concentration of salts and abrasive species in the seawater. Although SS has excellent mechanical strength and high corrosion-resistant properties, with those highly corrosive and abrasive environments exposed for a long time, various corrosion and wear attacks are inevitable. A denting phenomenon in the steam generator, cavitation erosion, erosion-corrosion in the turbine blades, general corrosion and pitting corrosion in the seawater lift pump, and Stress Corrosion Cracking (SCC) in the various pipes are the representative problems.

To improve the corrosion resistance of SS, the nanoporous oxide layer on the SS surface was previously studied. Actual improvement was available with such a method and it was verified with the electrochemical analysis including polarization curve and impedance spectroscopy. However, the long period of contact of the nanoporous oxide layer with aggressive seawater eventually let the corrosive species penetrate the protective layer. The pores that mitigated the volume expansion stress of the growing oxide layer, were treated as penetration routes for corrosive elements. Therefore, when the concentration of corrosive species exceeds a certain threshold limit, corrosion attacks were induced after all.

In this paper, to solve the aforementioned problems, plasma electrolysis was conducted. Among that electrolysis, specifically, Cathodic Plasma Electrolytic Oxidation (CPEO) was utilized. The CPEO process uses extremely high pulsed voltages and temperatures to form a protective layer on the substrate. Generally, the CPEO process shows a loose outer layer and an inner compact layer with great hardness and adhesion. Due to the absence of a possible penetration route for corrosive species, all the aggressive elements are blocked efficiently and protection from the wear attacks can be also achieved. Therefore, after fabricating the compact and protective oxide layer on the SS using CPEO, various characterizations were conducted to analyze the exact composition and structure of the oxide layer as well as its protectiveness against corrosion attack. With those closer inspections of the oxide layer, further improvements are expected which can contribute to developments in the corrosion resistance of structural materials.

2. Methodology

2.1 Materials and characterization

A specially designed SS specimen was used for the CPEO experiment (Fig. 1). The specimen had a circular part targeting the CPEO and a handle part for the electrical connection. The 316 type SS was used which had a composition of 17 % Cr, 12 % Ni, 2.5 % Mo, 0.08 % C, and the balance being Fe. In the case of electrolyte, 80 vol% glycerol (ACS reagent, ≥ 99.5 %) solution was used and 0.5 M KCl (ACS reagent, 99.0-100.5 %) was used as a conductive material. Before the CEPO process, the sample was electropolished to evenly disperse the electric field among the surface during CPEO. The electropolishing agent was composed of phosphoric and sulfuric acid with 50 vol % each, and the temperature of the electrolyte was maintained at 75 ℃. By applying 0.15 A/cm^2 for 15 min, samples were sonicated in acetone and DI water for 10 min separately. Finally, the samples were dried in an oven at 50 ℃.

Figure 1. Type 316 stainless steel specimen

After the CPEO experiment, the morphology characterization was conducted using a field emission scanning electron microscope (FESEM, Hitachi SU5000, Japan), and cross-sectional composition was characterized with the SEM-attached Energy Dispersive X-ray Spectroscopy (EDX). The crystalline structure and composition of the specimen were examined using an X-ray diffractometer (XRD, D/MAX 2500 V, Rigaku, Japan), X-ray photoelectron spectroscopy (XPS, Nexsa G2, Thermo Scientific, USA), and Fourier Transform Infrared Spectrometer (FT-IR, Nicolet iS50, Thermo Fisher Scientific Instrument, USA). Finally, the electrochemical corrosion test was conducted using a three-electrode system connected to a potentiostat (Biologic, SP-200). The electrolyte for the corrosion test was artificial seawater, and Pt sheet, and Ag/AgCl electrodes were used as the counter, and reference electrodes. The corrosion parameters were recorded in the range of -0.25-0.5 V with a rate of 50 mV/min.

2.2 Cathodic Plasma Electrolytic Oxidation (CPEO)

In general, Plasma Electrolytic Oxidation (PEO) technique is applied only to the valve metals, such as Aluminum, Zirconium, Magnesium, etc. However, plasma discharges on the SS surface hardly occur owing to the absence of stable insulating film formed on the surface and the lower oxidation driving force of the iron compared to that of hydrogen. To compensate for these problems, a Cathodic Plasma Electrolytic Oxidation (CPEO) was conducted. The SS target was placed as a cathode and the evolved gas-phase envelope on the surface was used as the insulating film for the plasma discharges with the appearance of breakdown. Among those gas phase activated elements, active species such as active oxygen or carbon contents are combined with the surface-active metals to form oxides. Fig. 2a shows the schematic diagram of the CPEO process, and Fig. 2b shows the experimental setup of the CPEO process.

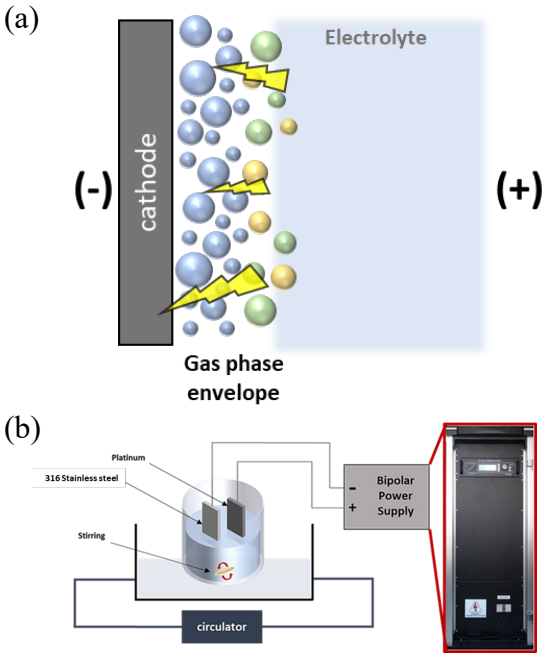

Figure 2. Schematic diagram of CPEO(a) and experimental setup (b)

The electrolyte, which was mentioned in the previous part, was maintained at 5 ℃ using a glass jacketed beaker, and stirring was performed during the CPEO process. A pulsed DC voltage of 600 V was forced to the electropolished SS 316 sample with a 10 % duty cycle and frequency of 100 Hz for 30 s. After the process, the samples were rinsed with ethanol and dried in an oven at 50 ℃.

3. Results and Discussion

3.1 morphology and composition

After the CPEO experiment of 30 s duration, the surface morphology was characterized with FESEM equipment. By polishing the sample with 400, 1000, 2000, 4000, and 7000 grit papers, a cross-sectional image was also obtained. As shown in Fig. 3 (a), the surface morphology showed noticeable grains with a small number of pores. Those pores can be interpreted as the traces of the plasma discharge channel resulting in a thick oxide layer. As well known, SS is an alloy composed of various metals. Therefore, metals that have different diffusion coefficients interact with active oxygen elements on the surface with different frequencies. Then the fabricated oxide layer turns out to be layer by layer shape with different compositions by each layer. Recognizing the characteristics, as shown in Fig. 3 (b), it can be seen that the oxide layer is composed of two different types. One with a porous and loose structure at the top, and the other with a compact structure at the bottom. The thickness of the total oxide

layer was estimated at 18.5 μm. The interesting part of its layer-by-layer structure was found at the bottom compact layer. The inner compact layer showed a inter-diffusion like morphology, which was gradually changed to a metal substrate as it deepens. The upper part of the inner layer showed a compact shape, though, underneath the compact layer showed dots of oxides mixed with the SS substrate. The unique structure of the fabricated oxide layer is expected to provide excellent adhesiveness with the CPEO process.

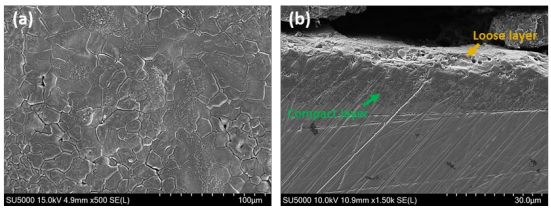

Figure 3. Surface (a), and cross-sectional (b) morphologies of 30 s CPEO processed 316 SS sample

As shown in Fig.4 (a), it can be deduced that the loose layer on the top was mainly composed of Fe oxides, and a small amount of Cr was also detected, which is can be placed below those Fe oxides. From the cross-sectional view (Fig. 4 (b)), it can be noticed that the inner compact layer was fully composed of Cr oxides while the loose layer on the top was again demonstrated as Fe oxides. The strong diffusion tendency of Fe compared to that of Cr might have caused this specific morphology.

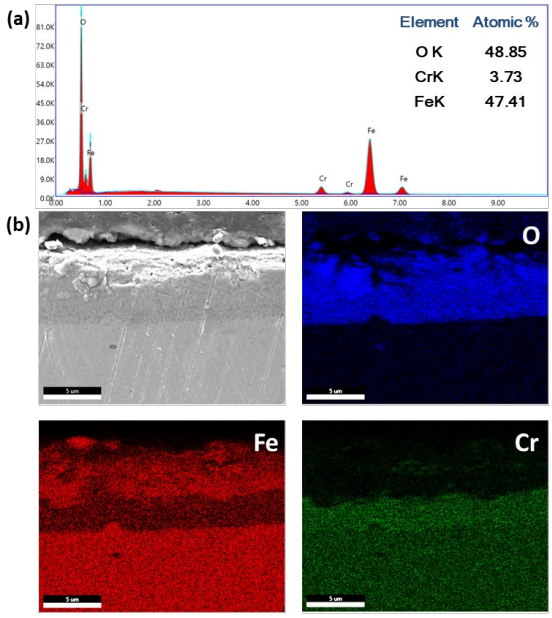

Figure 4. Surface EDS spectrum (a), and cross-sectional EDS mapping (b) of 30 s CPEO processed 316 SS sample

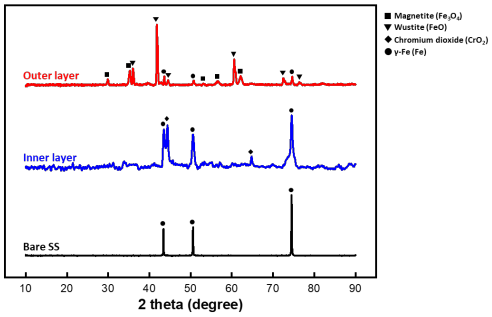

Figure 5. XRD patterns of 30 s CPEO processed 316 SS sample

For a closer look at the crystalline structure of the fabricated oxide layer, XRD characterization was firstly performed. To analyze the two separate layers, after detecting the outer layer first, the sample was carefully polished to reveal the inner layer. By doing so, it was possible to obtain the crystalline structures of each layer. In Fig. 5, it can be seen that the outer layer was mainly composed of Magnetite (Fe_3O_4) and Wüstite (FeO). Also, a small amount of γ-Fe was detected which came from the SS substrate. In the case of an inner layer, Chromium dioxide was mainly fabricated with the stronger peak of γ-Fe. These tendencies were in consent with the aforementioned EDS mapping results.

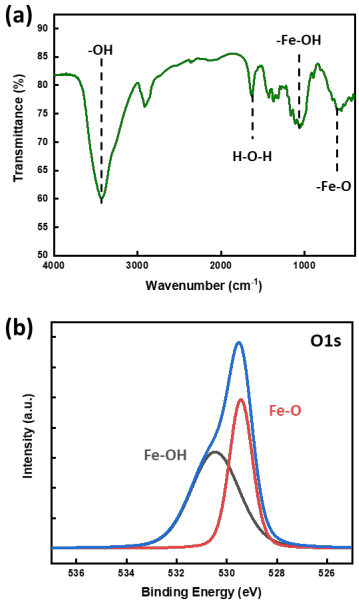

Figure 6. FT-IR (a), and XPS (b) spectrum of 30 s CPEO processed 316 SS sample

To analyze the oxide layer fabricated, FT-IR was also conducted and the result is shown in Fig. 6 (a). Interestingly, other than the oxygen bonding which forms the Magnetite or Wüstite, OH bonding was

simultaneously detected. From such a result, it can be expected that the FeOOH with a small amount was formed on the surface of the CPEO sample. The quantity of OH bonding that is spread through the surface can be considerably small resulting in the absence of an XRD peak. Additional characterization with XPS (Fig. 6(b)) equipment also supported the existence of FeOOH through O1s peaks. The strong oxygen peak was deconvoluted into two peaks of O^{2-} and OH^{-}. Comparing the OH- peak area with other references, it was reasonable to decide that the FeOOH was formed.

3.2 Corrosion resistance

The corrosion resistance of the bare SS and CPEO sample was characterized using the potentiodynamic polarization technique. Mainly corrosion potential and current were analyzed with the polarization curve. The corrosion potential is a coinciding potential between the oxidation and reduction reaction which refers to the environmental susceptibility to corrosion attacks. In the case of corrosion current, it refers to an absolute amount of corrosion occurring in the sample. By looking at the polarization curve in Fig. 7, it can be noticed that the CPEO sample curve is placed below compared to the bare SS curve which means the CPEO sample showed lower corrosion current. By tafel fitting the curves, the significant values of corrosion potential and the current were obtained and organized in table 1. The corrosion current value of the CPEO sample was significantly lower compared to the bare sample. Approximately 68 % decrease was reported mentioning a small amount of corrosion occurring. However, from the corrosion potential point of view, it was found that the CPEO sample showed more negative potential. With the negative shift of the corrosion potential, it can be interpreted that the CPEO sample is more susceptible to corrosion attacks in a given artificial seawater environment. Previously mentioned FeOOH formation on the surface can be the main reason for this negative shift of potential. Those OH bondings accelerated and trapped the corrosive solution on the surface providing a higher chance of corrosion to the outer oxide layer. Due to the inner compact layer, the total corrosion amount occurring was lower, though, the sample went through a more susceptible environment for corrosion attacks. With further development of OH-free oxide layer fabrication by recrystallizing process, superior corrosion resistance oxide layer can be fabricated with CPEO process.

Table 1. Major corrosion parameters from the curves

	Bare	30 s
Corrosion potential (E_{corr}) / mV	-287.398	-444.568
Corrosion current (i_{corr}) / μA	4.119	1.318
Corrosion rate (mmpy)	3.735×10^{-3}	1.164×10^{-3}

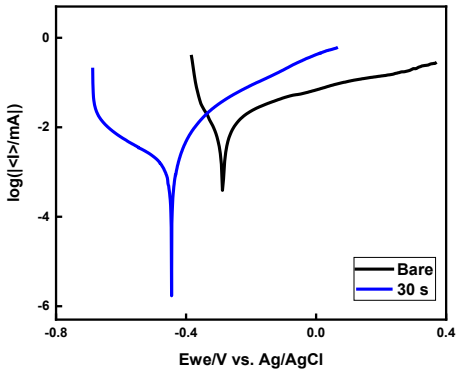

Figure 7. Potentiodynamic polarization curve comparison between bare and 30 s CPEO processed 316 SS sample

4. Conclusion

To improve the corrosion resistance of the main structural material (SS) for cooling water components, the CPEO process was tested for a short duration of 30 s. After the process, a thick oxide layer was fabricated on the surface of the SS. The oxide layer was composed of two different layers; the outer porous and loose layer which was mainly composed of Fe oxides and the inner compact layer composed of Cr oxides. Crystalline structure analysis found that the Fe oxides were made up of Magnetite and Wüstite and the inner Cr oxides were made up of Chromium dioxide. With XPS and FT-IR characterization, additionally, FeOOH was also detected on the outer surface of the oxide layer. The electrochemical test showed improved corrosion resistance with the CPEO sample showing a much lower corrosion current compared to the bare SS sample. However, the corrosion potential was negatively shifted with the CPEO sample indicating that the oxide layer formed was susceptible to corrosion attacks in a given testing condition. It is attributed to the formation of FeOOH at the outer surface which can trap the corrosive solution in the outer oxide layer. Regarding the much lower value of corrosion current which indicates the amount of corrosion event occurring, it can be concluded that the CPEO process can improve the corrosion resistance of the SS sample with compact inner oxide layer formation. Further development can be achieved by reducing the OH elements and recrystallizing the oxide layer. Therefore, the CPEO process will ultimately contribute to the related industrial fields.

REFERENCES

[1] Darband, Gh Barati, et al. "Plasma electrolytic oxidation of magnesium and its alloys: Mechanism, properties and applications." *Journal of Magnesium and Alloys* 5.1 (2017): 74-132.
[2] Clyne, Trevor William, and Samuel Christopher Troughton. "A review of recent work on discharge characteristics during plasma electrolytic oxidation of various metals." *International materials reviews* 64.3 (2019): 127-162.
[3] Yang, Xu, et al. "Cathodic plasma electrolysis processing for metal coating deposition." *Plasma Chemistry and Plasma Processing* 37.1 (2017): 177-187.
[4] Jin, Xiaoyue, et al. "Characterization of wear-resistant coatings on 304 stainless steel fabricated by cathodic plasma electrolytic oxidation." *Surface and coatings technology* 236 (2013): 22-28.
[5] Jin, Xiaoyue, et al. "Preparation and tribological behaviors of DLC/spinel composite film on 304 stainless steel formed by cathodic plasma electrolytic oxidation." *Surface and Coatings Technology* 338 (2018): 38-44.
[6] Tavares, Tássia Silva, et al. "Δ-FeOOH as support for immobilization peroxidase: optimization via a chemometric approach." Molecules 25.2 (2020): 259.
[7] Chagas, Poliane, et al. "δ-FeOOH: a superparamagnetic material for controlled heat release under AC magnetic field." Journal of nanoparticle research 15 (2013): 1-7.
[8] Heo, Jun, et al. "Improvement of corrosion resistance of stainless steel welded joint using a nanostructured oxide layer." Nanomaterials 11.4 (2021): 838.